A STUDY OF LUNAR IMPACT CRATER SIZE-DISTRIBUTIONS*

GERHARD NEUKUM** and BEATE KÖNIG
Max-Planck-Institut für Kernphysik, Heidelberg, F.R.G.

and

JAFAR ARKANI-HAMED**
Arya-Mehr University of Technology, Tehran, Iran

(Received 14 October, 1974)

Abstract. Discrepancies in published crater frequency data prompted this study of lunar crater distributions. Effects modifying production size distributions of impact craters such as surface lava flows, blanketing by ejecta, superposition, infilling, and abrasion of craters, mass wasting, and the contribution of secondary and volcanic craters are discussed. The resulting criteria have been applied in the determination of the size distributions of unmodified impact crater populations in selected lunar regions of different ages. The measured cumulative crater frequencies are used to obtain a general calibration size distribution curve by a normalization procedure. It is found that the lunar impact crater size distribution is largely constant in the size range 0.3 km $\leqslant D \leqslant$ 20 km for regions with formation ages between $\approx 3 \times 10^9$ yr and $\gtrsim 4 \times 10^9$ yr. A polynomial of 4th degree, valid in the size range 0.8 km $\leqslant D \leqslant$ 20 km, and a polynomial of 7th degree, valid in the size range 0.3 km $\leqslant D \leqslant$ $\leqslant$ 20 km, have been approximated to the logarithm of the cumulative crater frequency N as a function of the logarithm of crater diameter D. The resulting relationship can be expressed as $N \sim D^{\alpha(D)}$ where α is a function depending on D. This relationship allows the comparison of crater frequencies in different size ranges. Exponential relationships with constant α, commonly used in the literature, are shown to inadequately approximate the lunar impact crater size distribution. Deviations of measured size distributions from the calibration distribution are strongly suggestive of the existence of processes having modified the primary impact crater population.

1. Introduction

Most of the craters on the lunar surface are impact craters. This has become evident with the fundamental work by Baldwin (1949, 1963), Öpik (1960), and Shoemaker *et al.* (1962). The recent Apollo missions to the Moon have provided overwhelming confirmation of this view.

The measurement of crater frequencies in individual regions gives a means for determining relative surface age differences, the longer the exposure to impacts the higher the crater frequency. The possibility of determining the cratering chronology during the early existence of the Moon has been given by relating the crater frequencies of the Apollo Landing Sites to the radiometric ages of the respective lunar rocks. There exists relevant work on this topic by Shoemaker (1970), Baldwin (1971), Hartmann (1970, 1972), Soderblom and Boyce (1972), Bloch *et al.* (1971), and Neukum *et*

* The research reported in this paper was done in cooperation with the Planetology Program Office, NASA Headquarters, Washington D.C.
** A portion of the research reported in this paper was done while the first and the last author were Visiting Scientists at the Lunar Science Institute which is operated by the Universities Space Research Association under Contract No. NSR 09-051-001 with the National Aeronautics and Space Administration.

The Moon **12** (1975) 201–229.

al. (1972). We have learned that the cratering rate has decreased over several orders of magnitude during the first 1–1.5 billion years after the Moon's formation. This fact is of great importance for age determination: Very short periods of time show up in great crater frequency differences. There lies, however, still considerable uncertainty in the details of this flux decrease. A major source for error relates to the fact that different authors have determined inconsistent crater frequencies in the same or similar areas. Hartmann (1972) compares crater frequency data of different authors for the same sites and finds discrepancies up to a factor of 3. His method of averaging the different data seems to be an insufficient attempt to generalize crater frequency data because reasons for the discrepancies have not been studied. Uncertainties of a factor of 2 and more are too great because they would (with our present state of knowledge) lead to age errors of several hundred million years for lunar surface regions. Not even relative age differences could be determined reliably. Such uncertainties make practically useless age determinations by crater frequency measurements.

One obvious reason for discrepancies in interpreting crater frequency data is the fact that there exist different laws for the lunar crater size distributions maintained to be valid for partly the same size ranges (Shoemaker *et al.*, 1970; Baldwin, 1971; Hartmann and Wood, 1971). These laws are exponential relationship of the form $N \sim D^{\alpha}$, (N = cumulative crater frequency, D = crater diameter, α = constant). Chapman and Haefner (1971) have pointed out that such a simple law does not hold for a variation of D over a wider size range. Neukum *et al.* (1972) have come to the same conclusions that α is not constant, but is a function of crater diameter.

A detailed discussion of the form of the lunar crater size frequency distribution does not exist. A reliable determination of it is, however, necessary, because in the fewest cases it is possible to safely compare frequencies of equally sized craters in different regions, and thus a comparison of craters of different sizes is required. An extrapolation into unobserved diameter ranges on the basis of one of the quoted exponential laws is highly questionable.

In this paper, we study the form of lunar crater size distributions and their time development. Our goal is to find a general crater size frequency distribution for the lunar primary impact crater production populations. We discuss effects modifying lunar crater distributions, such as surface lava flows, blanketing by ejecta, superposition of craters, infilling and abrasion, mass wasting, and the contribution of secondary and volcanic craters to the primary populations. The reliability of other authors' data is questioned with respect to absolute crater frequencies and form of the distributions. In many cases, the above mentioned effects have not been accounted for, or are not clear. Additionally, some data are hardly usable because they are not given in tabular form with errors. That is why we purposely use only our own measurements in most cases.

2. Effects of Local Processes on Lunar Crater Populations

Let us assume that we have a fresh surface area on the Moon. This area will be cratered

with time. A crater population with a certain size distribution builds up. If no craters are destroyed by superposition, ejecta blanketing and similar cratering processes, and if no other non-cratering processes (as e.g. destruction of craters by lava flows) are working, this crater population will not change its size distribution. After a certain interval of time, the frequency will be enhanced by the same amount at *any* crater size, i.e. the ratio of the frequencies at time t_1 and t_2, respectively, is solely a function of time independent of crater diameter! This picture holds only when the meteorite population whose image is the crater population on the Moon does not change its velocity-mass-distribution with time. This has to be verified in the real case of the lunar crater populations and is treated in Section V.

In reality, the lunar surface has been subject to many endogenic and exogenetic modifications. These modifications have interacted with pre-existing crater populations and changed their size distribution behaviors characteristically. The most effective processes are discussed in the following.

2.1. Flooding

Magmatic activity was a widespread phenomenon in the early lunar history (e.g., Schaber, 1973). All mare surfaces formed by lava extrusions. This process interacted with crater populations. Smaller craters are preferentially affected in a lava flooding process, and may completely vanish depending on flow thickness. Larger craters are flooded from outside analogous to terrestrial kipukas. These phenomena can be studied in the stereopair of Figure 1. The largest crater, Brayley C, is a member of the preflooding crater population. Its ejecta blanket has been buried by a lava that originated outside the crater. The crater left of it, Brayley E, formed after the last flows. Its ejecta blanket is not covered by any lava. South-west of this crater pair, left of the Rille, a group of small, km-sized craters is situated which have been flooded almost to their rim crests. Smaller pre-existing craters must have completely been flooded and cannot be seen any more.

As obvious, this process selectively influences a crater population. There is a relatively sharp boundary in crater size, below which craters are completely erased and above which craters are still existing and can be counted. If no difference is made between post-flooding craters and those whose ejecta blanket is flooded from outside, one finds size distribution behaviors as shown in Figure 2 for the Apollo 11 and 12 LS and Mare Smythii distributions. We obtain a distribution with this well-pronounced irregularity (Mare Smythii, Apollo 12 LS), if a major flooding process happened. For successive floodings with small time intervals between each other, the cumulative size distribution we observe today will show an overall flatter behavior as it is probably the fact for the population in the vicinity of Apollo 11 LS (Figure 2). These processes are discussed in detail by Neukum and Horn (1974).

2.2. Blanketing

The effects discussed above are similar in blanketing processes and have been treated mainly in this context by Hartmann and Wood (1971). Ejecta of very large craters,

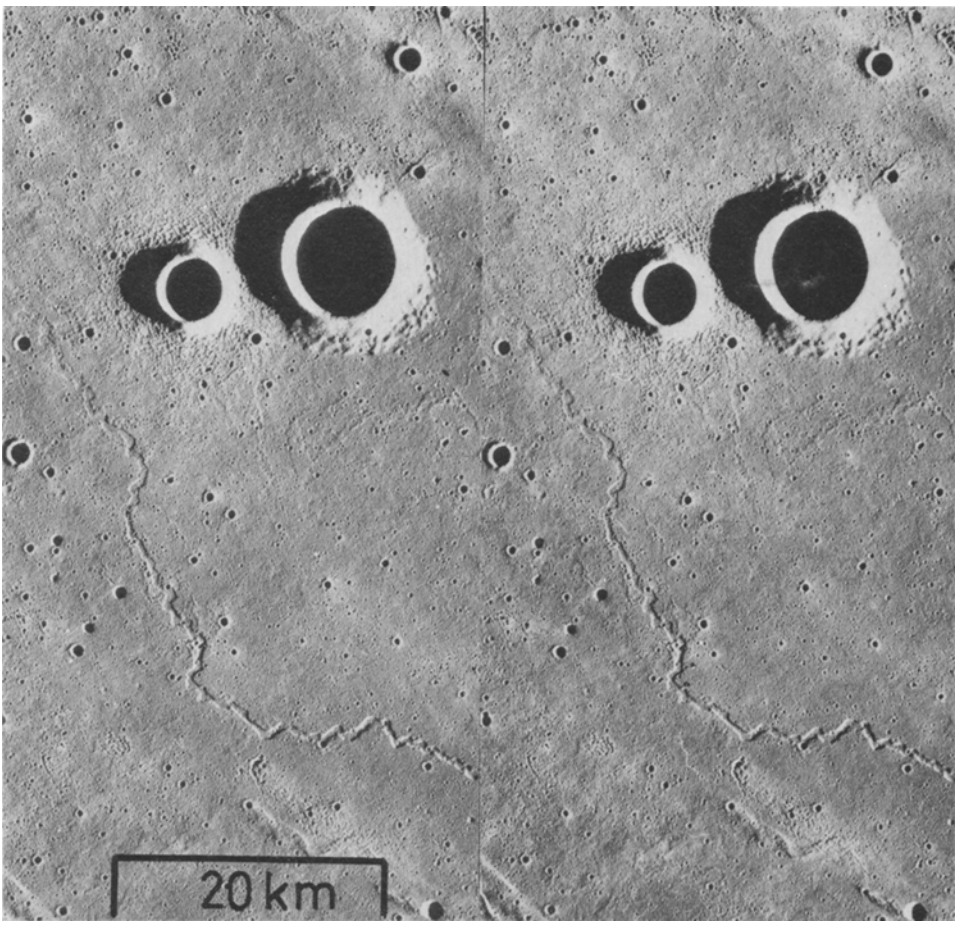

Fig. 1. Stereopair of an area in north-eastern Oceanus Procellarum around the craters Brayley C and Brayley E at approximately 39.5° W, 21° N (AS 17-2929; 2930 Metric). It shows the effect of lava flows on craters. Small craters are flooded up to their rim crests.

essentially the ringed basins, can blanket their surroundings hundreds of meters high depending on the distance from the center of impact (McGetchin *et al.*, 1973). Craters kilometers in size may be buried.

The size distributions of prexisting populations are affected in a way similar to flooding. The destruction conditions, however, are not so sharp. Ejecta blankets are often very discontinuous (Stöffler, 1974), and therefore smaller craters may survive by chance. Thus, a crater population which was subject to such an event will appear flattened similar to the case for successive thin flooding.

Probable examples of populations affected by blanketing are those of the Apollo 14 LS and Descartes Highlands, east of the Apollo 16 LS (Neukum and König, 1974).

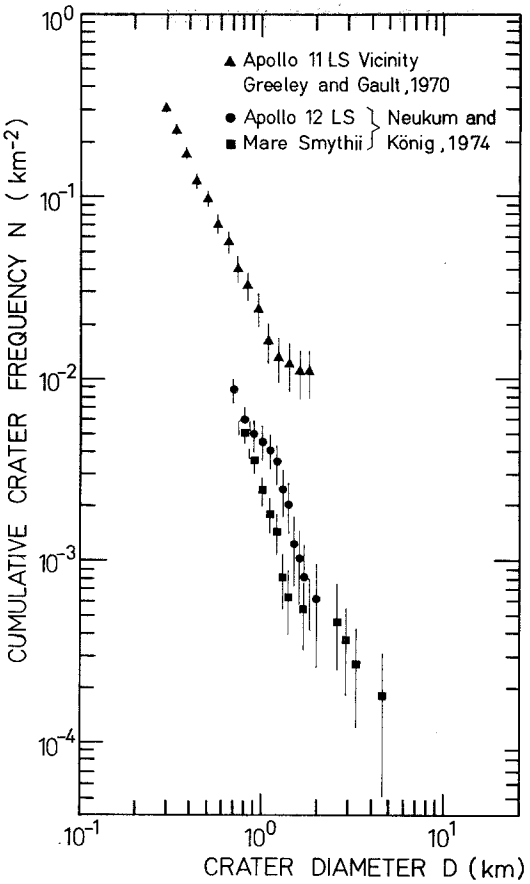

Fig. 2. Irregular size distributions of the Apollo 11 and 12 LS and Mare Smythii crater populations (from Neukum and König, 1974).

2.3. Secondary Cratering

Ejection of material during an impact causes the formation of secondary craters, as well seen by the presence of strewn fields of small craters around large recent lunar craters. Oberbeck and Morrison (1974) have investigated the formation of secondary craters in the laboratory and compared with lunar forms. They have studied characteristics of secondary craters which form crater chains, are often elongated approximately radial to the primary source crater, and are mostly flatter than primary ones. The best marking for identification is the herringbone pattern which occurs in simultaneous multiple secondary impacts.

On the basis of Oberbeck and Morrison's work one can exclude secondary craters in many cases. The distinction between primary and secondary craters is however not in all cases clear, especially if secondary craters do not occur in chains, but as isolated single craters. Thus, in the vicinity of large strewn fields of primary impacts a contribu-

tion of secondary craters to the primary population can be significant. It is in any case advantageous not to measure near those strewn fields or at least confine to sufficiently large craters because of the existing upper limit in the sizes of the secondary craters relative to the size of the primary source.

2.4. Superposition, infilling and abrasion

After a sufficient long time of exposure, when the crater frequency becomes high, new impacts destroy pre-existing craters by superposition. Gradual abrasion by smaller impacts and infilling by ejecta is another mechanism of crater destruction. The smallest craters are affected first because they are the most frequent, interact with each other and can efficiently be destroyed by few large impacts. Moore (1964), Trask (1966) and Shoemaker *et al.* (1970) have investigated lunar crater populations to study this process. Gault (1970) has performed laboratory studies simulating these crater destruction processes. Various authors have theoretically treated the development of a crater population affected by superposition, infilling and abrasion (Marcus, 1964, 1966; Walker, 1967; Soderblom, 1970; Neukum and Dietzel, 1971). All these studies result

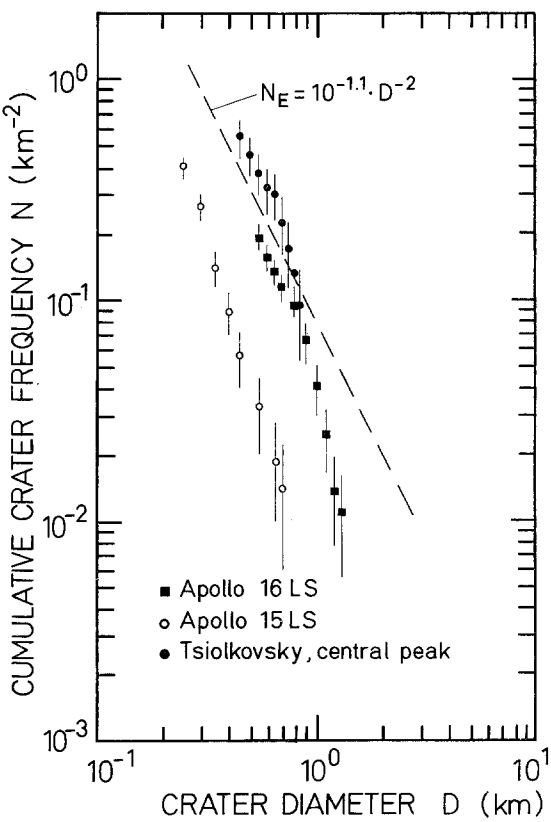

Fig. 3. Examples of size distributions which have approached the state of equilibrium. The equilibrium distribution (N_E) derived by Trask (1966) is given for comparison.

in a size distribution which has approached a state of equilibrium (i.e. independent of time) and whose frequency N_E follows the law $N_E \sim D^{-2}$. Inherent in this relation are some assumptions of the form of the production distribution which seem to be approximately met by the form of the production crater populations on the Moon. We do not want to discuss these problems in detail but want to show some examples of crater populations which have obviously approached this state of equilibrium. In Figure 3 the size distributions for the Apollo 15 LS (cf. Section 3), Apollo 16 LS, and crater Tsiolkovsky (central park) (Neukum and König, 1974) are displayed. The youngest population of the Apollo 15 LS has not yet reached equilibrium but is completely in production in the size range measured. The older population of Apollo 16 LS and Tsiolkovsky have approached equilibrium for craters with diameters $\lesssim 0.8$ km. The steep production populations have bent over to the characteristic D^{-2}-distribution and approximately follow the equilibrium relationship given by Trask (1966).

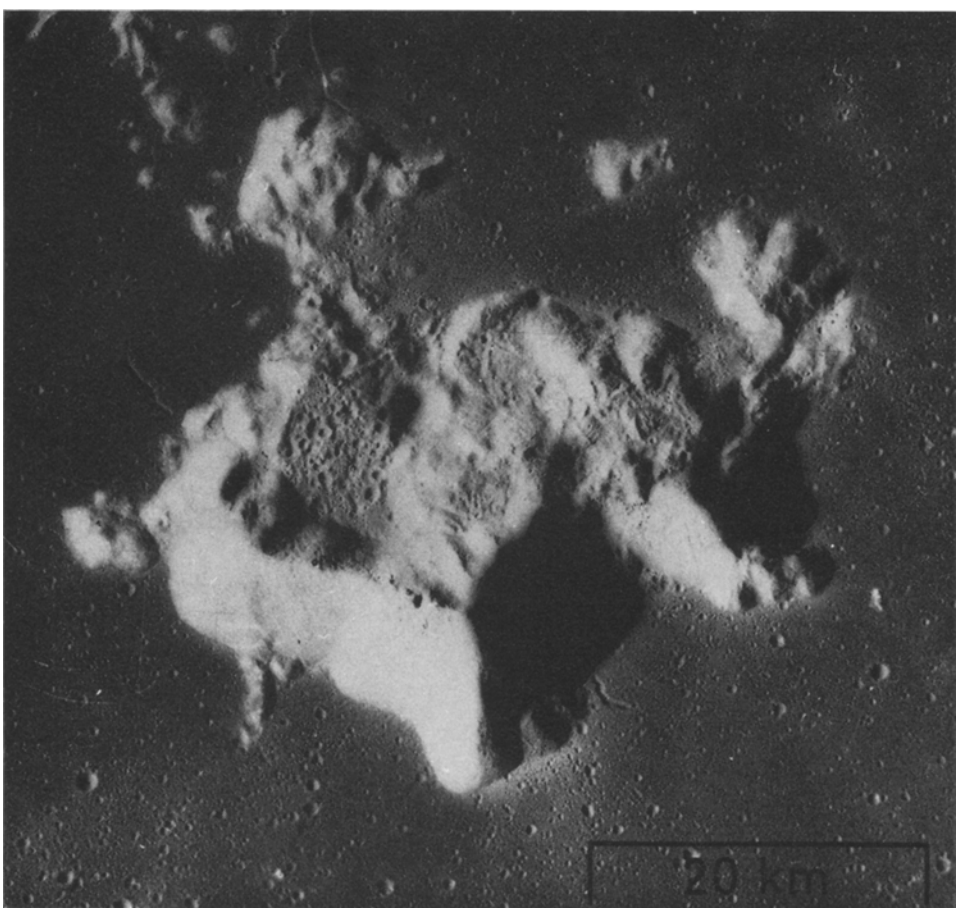

Fig. 4. Central peak of cretar Tsiolkovsky (128.5°E, 20°S). Steep slopes do not show any craters because of mass wasting (AS 15-1030 Metric).

For comparison of frequencies in order to obtain age differences one must confine to the part of the distribution representing craters still in production, i.e. to the larger craters.

2.5. Mass wasting

An efficient process destroying craters is mass wasting. Craters formed on slopes will gradually be erased by landslides. That is why we do not see many craters on oblique areas on the Moon. Additionally, craters at the foot of the slopes will be covered by the debris. Small impacts will help in triggering and amplifying those processes.

A good example to illustrate these conditions is the central peak in crater Tsiolkovsky (Figure 4). The nearly level small plateau on the peak shows numerous craters, but there are none of the steeper slopes of the peak.

What size of craters is affected by mass wasting depends on the relief of the terrain. Craters smaller than the average relief will not quantitatively record, larger craters will negligibly be affected.

2.6. Volcanic craters

A small percentage of lunar craters is obviously of endogenic origin. They occur frequently in lunar rilles or grabens. Therefore, volcanic craters can in most cases be eliminated from the primary population. A detailed discussion of the frequency and occurrence of endogenic craters is given by Grudewicz (1973).

All these effects discussed under Section 2.2–2.6 have been kept in mind when looking for appropriate areas for determining unaffected primary impact crater production distributions for different aged regions of the lunar surface. We have looked for areas which seem homogeneous and do not show any signs of the discussed processes affecting the primary distributions.

3. Crater Frequency Measurements

3.1. Data acquisition and reduction

Craters were measured with two different facilities, (1) a device for monoscopic measuring on enlarged transparent photographs, and (2) a Zeiss 'Stereokomparator' for stereoscopic measurements.

The photographic material used for the monoscopic measurements was Lunar Orbiter and Apollo Metric positive transparencies which were enlarged up to 5 times. The stereoscopic measurements were done on Apollo Metric positive transparencies of original size or enlarged by a factor of 2.

The photographs were assumed to be taken really vertical which they are sufficiently close. The scales for the photos were determined through the respective photo support data in connection with the laser altimeter measurements by Kaula *et al.* (1973). The scales were cross-checked by comparing with the LAC charts (1962) and the Lunar Planning Chart (1972). We found discrepancies up to 3% when comparing the scales obtained through the orbit support data with the LAC charts, though practically none

($<1\%$) comparing with the Lunar Planning Chart. Our measurements are based on the scale determination through the respective photo support data.

In the monoscopic measurements, the crater diameters were usually measured in east-west-direction, from the inner shadow margin to the outer one. This procedure is practically equivalent to a rim-to-rim measurement. The measurement was done by tangentially applying a thin (≈ 0.1 mm) wire to the crater images. No craters smaller than 2 mm were measured. Thus, a possible systematic error caused by the finite thickness of the wire is $\lesssim 5\%$ depending on size of crater measured. It is supposed to average out and become smaller. In cases where the craters were obviously not circular, average diameters were measured by also considering the diameters in north-south-direction and taking an arithmetic means of both measurements.

In the stereoscopic measurements real rim-to-rim diameters were measured. The floating mark was set down on the rim at its highest points usually in east-west direction. Non-circular craters were averaged out as described above. The measurement accuracy of the device is 5 μ. In all cases, the uncertainty in diameter determination is $<2\%$.

The diameter measurements were automatically punched on cards in the measuring process. The data were computer processed. The craters measured were sorted according to their sizes and their numbers stored in the respective size intervals with a step width of 100 m. Cumulative crater frequencies and the respective statistical errors were calculated. The cumulative frequency is the number of craters per unit area, with diameters larger than z lower limit crater diameter D. In the computer processing, the cumulative crater frequency was calculated for the lower limit of every size interval, i.e. every 100 m. The statistical error is equal to the square root out of the cumulative number.

It is necessary here to discuss the usage of the method of cumulative frequencies instead of incremental ones. Chapman and Haefner (1967) have brought forward arguments against the cumulative method and favored the incremental one. They argue that the form of the cumulative crater size distribution cannot be determined in a well-defined way because of the propagation of the error of the incremental distribution. It is correct that the error propagates but is not relevant for the cumulative distribution. Additionally, the incremental method does not give any advantage in reality. This will be shown in the following. Mathematically the two methods are related by the equation

$$N(D) = \int_{D}^{\infty} n(D')\,\mathrm{d}D',$$

where N and n are the cumulative resp. differential frequencies, D the lower crater diameter limit. In the crater counting process the above integral relationship is replaced by summation over craters of different discrete sizes. The incremental frequency is $\mathrm{d}N = n(D)\,\mathrm{d}D$ which can be approximated by $\delta N = n(D)\,\delta D$. This means that in a

small interval δD the number of craters δN is measured to determine the immanent differential frequency $n(D)$ which is a fixed quantity related to the original size-velocity-distribution of the crater forming bodies. If δD is small, $n(D)$ is approximately constant for a variation of D over δD. Since then $\delta D \sim \delta N$, the statistical error in δN becomes large with smaller δD. If δD is chosen large, the statistical error in δN becomes small. However, the relationship $\delta N = n(D)\ \delta D$ does not hold any more; and $n(D)$ cannot then be sufficiently determined. The number of craters on a certain area A is proportional to A for a certain age of the area. In taking large counting areas conditions will be improved. In reality, however, this is seldom possible, because large areas with isotropic primary crater distribution are rare. Thus $n(D)$ can usually be defined only badly by measuring incremental frequencies.

On the other hand, we are interested in comparing absolute frequencies with each other. Any statistical variation for large craters which are rare does not interest in the comparison of absolute numbers for much smaller sizes. Additionally, the cumulative method is sensitive enough that irregularities in the frequencies show sufficiently well up as discussed before.

We agree with Öpik (1960) that the cumulative method is the appropriate method for comparing crater frequencies with each other. The incremental method can of course reveal fine details in the distribution of crater sizes. It should be applied to frequency measurements in very large areas with remarkably good statistics. However, we have not done so in our studies, though it is possible, because of the danger of over-interpreting the data.

3.2. Comparison of monoscopic and stereoscopic measurements

The Apollo 15 LS region has been investigated both in monoscopic and stereoscopic mode. The cumulative frequencies are shown in Figure 5. Both kinds of measurements agree well. The deviation for the larger craters is due to the fact that in the stereoscopic measurements, contrary to the monoscopic measurements 2 craters have been included which lie on a hilly area right of Hadley Rille. This area is indicated in the schematic draft in Table I (hatched). These craters may be 'pre-mare' ones.

As also described by Neukum and König (1974) a good agreement between stereoscopic and monoscopic measurements seems to be the case throughout, if the terrain is smooth and if the craters are unmodified by extensive flooding, mantling or blanket ing or too much eroded. In rough terrains, however, like the Apennines, stereoscopic measurements are mandatory if craters as small as 2 km or smaller are to be measured. One should always pre-inspect the investigated regions stereoscopically if photo material is available. Then, it can be decided whether steroscopic measurements are necessary or monoscopic measurements suffice.

3.3. Data

In the following Table I you see the crater frequency measurements of the lunar regions chosen for obtaining primary unmodified lunar crater populations.

The data are given in tabular form to make it easy for other workers in this field to

use them. The cumulative number N per km^2 (=cumulative frequency) of craters of diameters $\geqslant D$ is given together with the 1σ statistical error ΔN. The areas where counted can be localized on the Moon by using the schematic drawings additionally given for each region. The regions have been given identification numbers according to the pictures used in counting and where they have been localized. An additional subgroup number separated by a comma from the main location number refers to separate areas at the sites. Supplementary information, such as size of the areas, total number of craters counted and mode of measurement is given in the respective head descriptions. The sun angle is low in all measurements except for those of Mare Crisium. A high sun angle, however, is not critical for measurements of craters with diameters larger than 0.8 km.

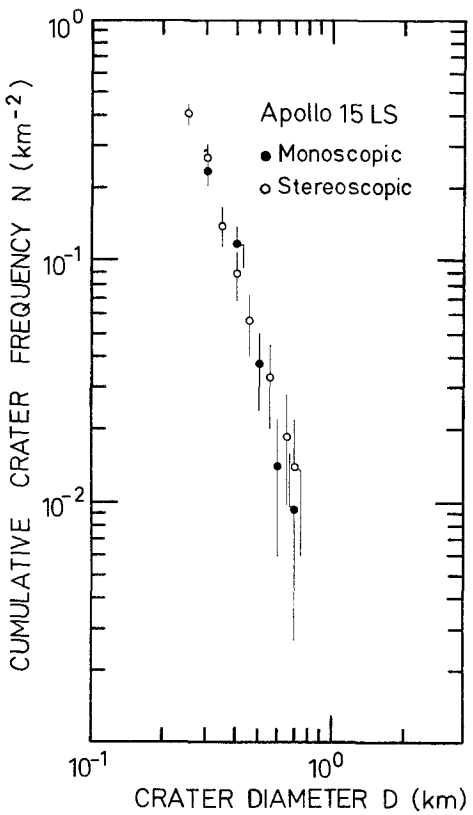

Fig. 5. Comparison of monoscopic and stereoscopic measurements at the Apollo 15 Landing Site.

TABLE I

Mare Serenitatis, Light Interior

Photo Material:

AS 15-396; 400; 404; 408; 2037; 1663; 2035; 2033; 1660; 1666

Area: 142621 km²

Total Counts: 1349

Mode of Measurement:
Monoscopic after stereoscopic inspection

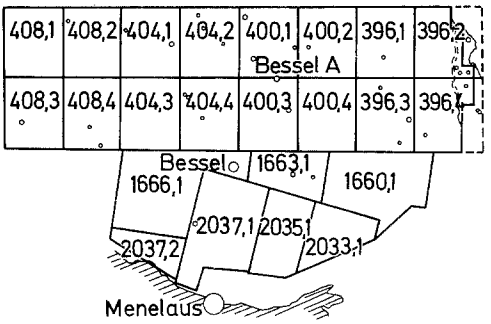

D(km)	N(km^{-2})	ΔN(km^{-2})	D(km)	N(km^{-2})	ΔN(km)$^{-2}$
0.8	9.46×10^{-3}	2.58×10^{-4}	2.5	1.47×10^{-5}	3.21×10^{-6}
0.9	6.10	2.07	2.6	1.26	2.97
1.0	3.91	1.65	2.7	1.19	2.89
1.1	2.63	1.36	2.8	1.12	2.80
1.2	1.84	1.14	2.9	9.82	2.62
1.3	1.30	9.54×10^{-5}	3.1	8.41	2.43
1.4	9.61×10^{-4}	8.21	3.3	7.71	2.33
1.5	7.15	7.08	3.6	7.01	2.22
1.6	5.75	6.35	3.8	6.31	2.10
1.7	4.49	5.61	4.5	5.61	1.98
1.8	3.79	5.15	4.6	4.91	1.86
1.9	3.58	5.01	5.0	4.21	1.72
2.0	2.94	4.54	5.5	3.51	1.57
2.1	25.9	4.26	5.6	2.80	1.40
2.2	2.43	4.15	6.1	2.10	1.21
2.3	2.03	3.78	7.5	1.40	9.92
2.4	1.96	3.71	15.5	7.01×10^{-6}	6.31

Mare Crisium, Eastern Part

Area: 44109 km²

Photo Material:
AS 17-423; 424; 426; 427; 428

Total Counts: 250

Mode of Measurement:
Monoscopic

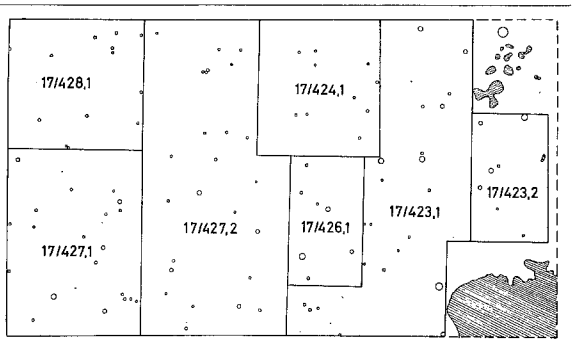

D(km)	N(km^{-2})	ΔN(km^{-2})	D(km)	N(km^{-2})	ΔN(km^{-2})
0.8	5.67×10^{-3}	0.36×10^{-3}	1.8	4.31	0.99
0.9	3.74	0.29	1.9	3.17	0.85
1.0	2.63	0.24	2.2	2.49	0.75
1.1	1.93	0.21	2.3	1.81	0.64
1.2	1.34	0.17	2.4	1.59	0.60
1.3	1.02	0.15	2.6	1.13	0.51
1.4	7.71×10^{-4}	1.32×10^{-4}	2.9	0.91	0.45
1.5	5.44	1.11	3.1	0.45	0.32
1.6	4.99	1.06	3.6	0.23	0.23

Apennines

1. Total

Photomaterial:
AS 17-1819; 1820; 1822; 1823; 1825; 1826
AS 15-412; 413

Area: 37198 km²

Total Counts: 88

Mode of measurement:
Stereoscopic

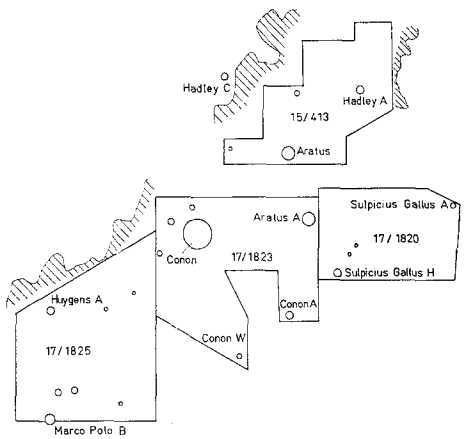

D(km)	N (km^{-2})	ΔN (km^{-2})	D(km)	N (km^{-2})	ΔN (km^{-2})
2.0	2.37×10^{-3}	0.25×10^{-3}	3.9	4.57	1.11
2.1	2.02	0.23	4.2	4.30	1.08
2.2	1.77	0.22	4.3	4.03	1.04
2.3	1.67	0.21	4.5	3.76	1.01
2.4	1.48	0.20	5.0	3.23	0.93
2.5	1.32	0.19	5.1	2.96	0.89
2.6	1.18	0.18	5.5	2.69	0.85
2.7	1.13	0.17	5.9	2.42	0.81
2.8	1.05	0.17	6.0	2.15	0.76
2.9	9.68×10^{-4}	1.61×10^{-4}	6.2	1.88	0.71
3.0	9.14	1.57	6.4	1.61	0.66
3.1	8.06	1.47	6.5	1.34	0.60
3.2	6.72	1.34	6.6	1.08	0.54
3.3	6.45	1.32	9.2	8.06×10^{-5}	4.66×10^{-5}
3.6	6.18	1.29	10.2	5.38	3.80
3.7	5.65	1.23	21.4	2.69	2.69
3.8	5.11	1.57			

Apennines

2. Region 15/413:

Photo Material: AS 15-412; 413

Area: 8009 km²

Total Counts: 70

Mode of measurement: Stereoscopic

D(km)	N (km^{-2})	ΔN (km^{-2})	D(km)	N (km^{-2})	ΔN (km^{-2})
1.4	7.24×10^{-3}	0.95×10^{-3}	2.4	1.25	0.39
1.5	5.74	0.85	3.0	9.99×10^{-4}	3.53×10^{-4}
1.6	5.24	0.81	3.6	8.74	3.30
1.7	4.00	0.71	4.2	7.49	3.06
1.8	3.25	0.64	4.3	6.24	2.79
1.9	3.12	0.62	4.5	4.99	2.50
2.0	2.37	0.54	5.0	3.75	2.16
2.1	2.00	0.50	6.6	2.50	1.77
2.2	1.62	0.45	10.2	1.25	1.25
2.3	1.37	0.41			

Table I (Continued)

Apollo 16 Landing Site, Light Plains

Photo Material: AS 16-440

Area: 3755 km²

Total Counts: 87

Mode of measurement:
Monoscopic after stereoscopic inspection

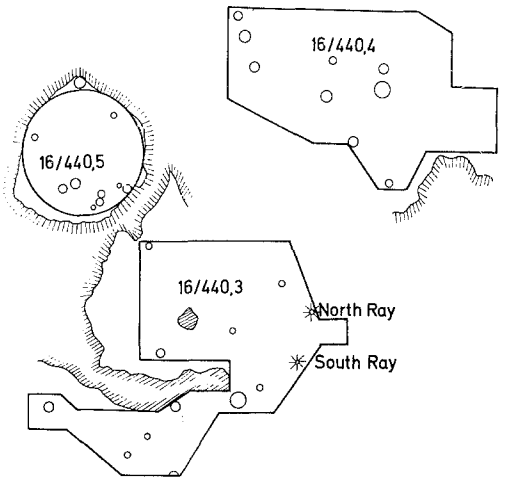

D(km)	N (km^{-2})	ΔN (km^{-2})	D(km)	N (km^{-2})	ΔN (km^{-2})
1.1	2.32×10^{-2}	0.25×10^{-2}	2.0	–	–
1.2	1.68	0.21	2.1	2.93	0.88
1.3	1.28	0.18	2.2	–	–
1.4	9.06×10^{-3}	1.55×10^{-3}	2.3	2.13	0.75
1.5	6.92	1.36	2.4	1.60	0.65
1.6	5.86	1.25	2.5	1.33	0.60
1.7	4.53	1.10	2.8	0.80	0.46
1.8	3.73	1.00	3.4	0.53	0.38
1.9	3.20	0.92	3.5	0.27	0.27

Mendeleev

Area: 32 580 km²

Photo Material:
AS 16-344; 347

Total Counts: 102

Mode of measurement:

Monoscopic after stereoscopic inspection

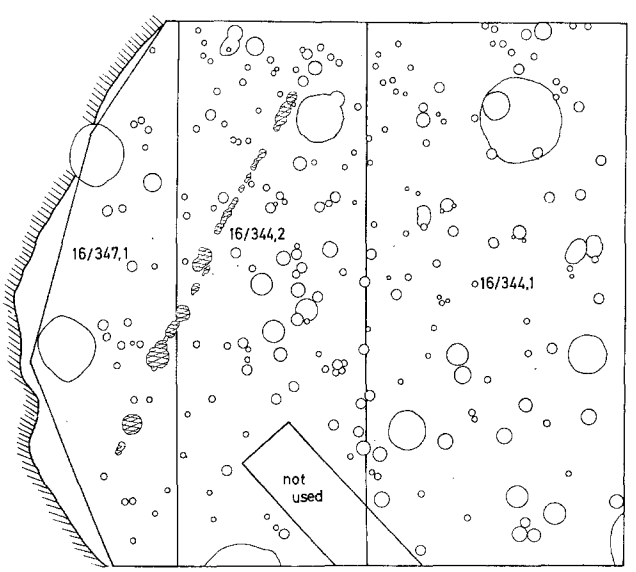

Table I (Continued)

D(km)	N(km^{-2})	ΔN(km^{-2})	D(km)	N(km^{-2})	ΔN(km^{-2})
3.0	3.13×10^{-3}	3.10×10^{-4}	5.2	7.98	1.57
3.1	2.76	2.91	5.4	7.67	1.53
3.2	2.67	2.86	5.6	7.06	1.47
3.3	2.55	2.80	6.0	6.14	1.37
3.5	2.27	2.65	6.1	5.52	1.30
3.6	2.03	2.49	7.0	4.91	1.23
3.7	1.90	2.42	7.8	3.99	1.11
3.8	1.81	2.36	7.9	3.68	1.06
3.9	1.53	2.17	8.1	3.38	1.02
4.0	1.38	2.06	8.4	3.07	9.71×10^{-5}
4.1	1.32	2.01	8.9	2.46	8.68
4.2	1.29	1.99	9.4	2.15	8.12
4.3	1.17	1.89	13.3	1.84	7.52×10^{-5}
4.4	1.14	1.87	14.0	1.53	6.86
4.5	1.10	1.84	16.2	1.23	6.14
4.6	1.07	1.82	20.4	9.21×10^{-5}	5.32
4.7	9.52×10^{-4}	1.71	21.0	6.14	4.34
4.8	8.59	1.62	28.3	3.07	2.76

Mare Orientale

Photo Material:
IV 195-H3; IV 194-H3;
IV 186-H3; IV 181-H1

Area: 61 254 km^2

Total Counts: 38

Mode of measurement:
Monoscopic

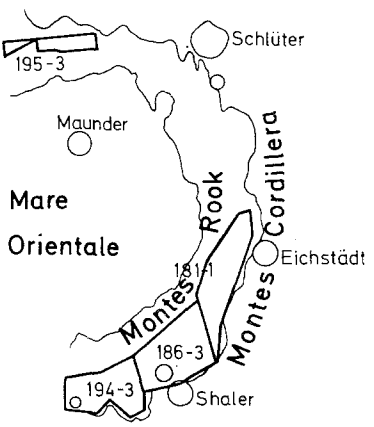

D(km)	N(km^{-2})	ΔN(km^{-2})	D(km)	N(km^{-2})	ΔN(km^{-2})
3.0	6.20×10^{-4}	1.01×10^{-4}	5.5	1.96	5.66
3.1	5.22	9.24×10^{-5}	5.6	1.80	5.41
3.2	4.73	8.79	5.7	1.63	5.16
3.4	3.93	8.00	5.9	1.47	4.90
3.6	3.75	7.83	6.2	1.31	4.62
3.7	3.59	7.66	6.9	1.14	4.32
3.8	3.43	7.48	7.1	9.80×10^{-5}	4.00
3.9	2.94	6.93	7.3	8.16	3.65
4.4	2.78	6.73	10.7	6.53	3.27
4.6	2.45	6.32	11.1	4.90	2.83
5.0	2.29	6.11	21.5	3.27	2.31
5.1	2.12	5.89	39.9	1.63	1.47

Table I (Continued)

Apollo 15 Landing Site

Photomaterial:
AS 15-413; 415

Area: 213 km²

Total Counts: 86

Mode of measurement:
Stereoscopic

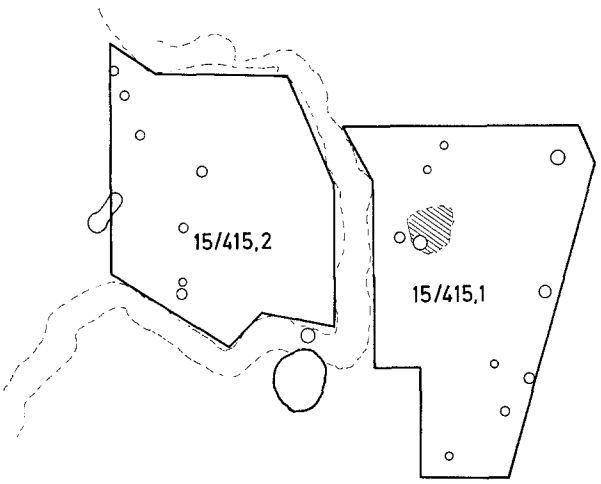

D(km)	N(km^{-2})	ΔN(km^{-2})	D(km)	N(km^{-2})	ΔN(km^{-2})
0.25	4.04×10^{-1}	0.44×10^{-1}	0.55	3.29	1.24
0.30	2.68	0.35	0.65	1.88	0.94
0.35	1.41	0.26	0.70	1.41	0.81
0.40	8.92×10^{-2}	2.05×10^{-2}	0.8	4.69×10^{-3}	4.69×10^{-3}
0.45	5.63	1.63			

4. Discussion of the Individual Crater Populations

In the following, we shall discuss the general appearance of the crater size distributions in the areas studied, discuss the measurements, and derive a calibration size distribution which allows the comparison of crater frequencies of different-sized craters on areas of different ages.

The effects described in Section 2 which influence lunar crater populations all tend to flatten the crater size distributions except the admixture of secondary craters. For obtaining unchanged primary populations, we chose homogeneous areas for scanning, according to the criteria described in Section 2, as far away from large secondary strewn fields as possible. Additionally, secondary craters have been eliminated in all counts in identifying them by the application of the criteria evaluated by Oberbeck and Morrison (1974). We may not have been able to eliminate all secondary craters, but as discussed in this section this will cause only negligible errors. The measurements presented in Table I are displayed in Figure 6. Their characteristics will be discussed in the following.

4.1. Mare Serenitatis

The light interior of Mare Serenitatis seems to be homogeneous. By visual inspection it has a relatively low crater density. Apollo 15 metric photography of sufficiently

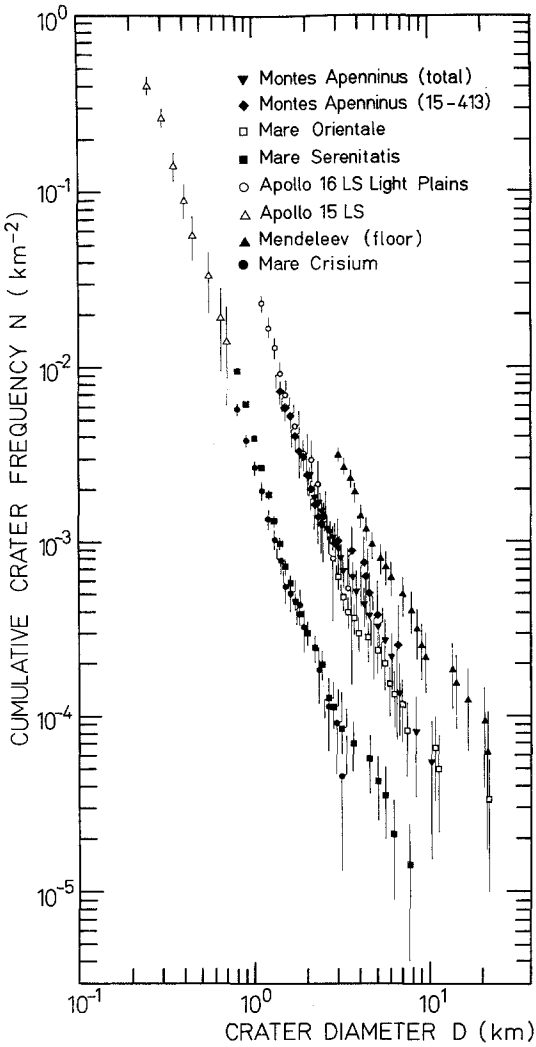

Fig. 6. Absolute cumulative size-frequency distribution of all populations measured.

good quality has been used. It is one of the best younger areas to get a valid size distribution for craters in the size range from 800 m up to more than 5 km. The measurements have been performed monoscopically after stereoscopic inspection. The darker 'shelf' region has been avoided in the measurements because of obviously different (higher) age and because of the presence of a great number of endogenic craters. About two-thirds of Mare Serenitatis light interior was covered as to be seen in the schematic draft in Table I.

Two large craters, Menelaus and Bessel, may influence the primary populations by their strewn fields. Since not all secondary craters may have been recognized, we have purposely counted craters in rings and zones around Bessel without eliminating second-

ary craters by application of the herringbone criterion. Only clearly elongated depressions have been skipped. The location of the counting areas is shown in Figure 7. One can easily identify clusters of secondary craters, partly stemming from crater Menelaus in the south west just outside the picture. The size distributions and absolute frequencies are given in Figure 8. The farther the distance to Bessel the lower the crater frequency. The solid line represents the average frequency of the light interior of Mare Serenitatis. This frequency is approached with greater distance from Bessel. It falls even somewhat below the average lines which means that region 454,9 is slightly younger than the average mare. This behavior is interpreted to be due to an admixture of $\lesssim 30\%$ of secondary craters around 1 km in diameter, in the immediate vicinity of

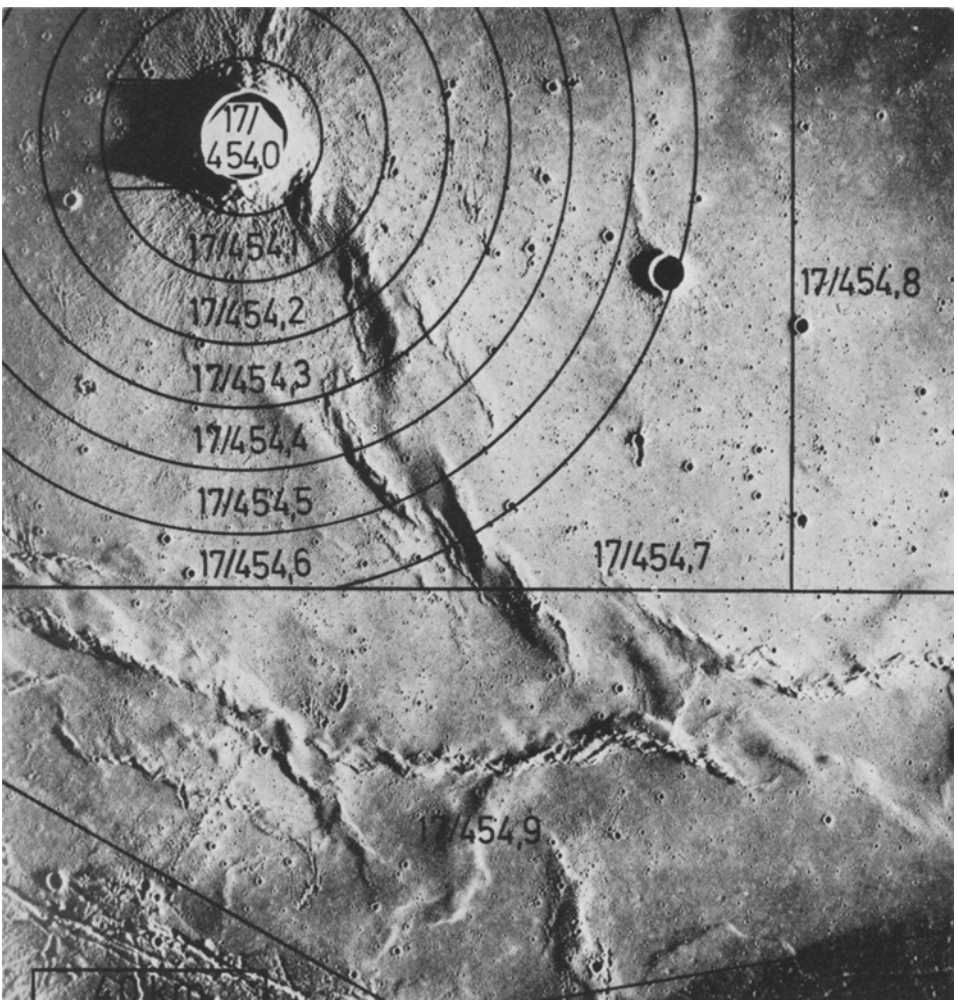

Fig. 7. Location of the counting areas around crater Bessel in Mare Serenitatis at 18° E, 22° N. Its strewn field is interfering with that of crater Menelaus in the South (outside picture) (AS 17-454 Metric).

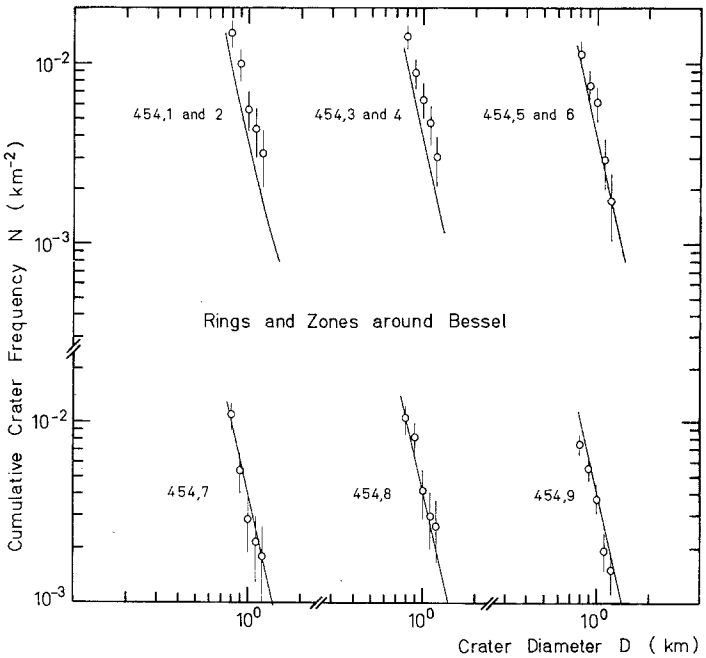

Fig. 8. Size-frequency distribution of the crater population in the counting areas around crater Bessel. The solid curve represents the average crater frequency of Mare Serenitatis.

Bessel, which rapidly falls down to almost zero at a distance of about 7 crater radii. The admixture of secondary craters with diameters >1.5 km is negligible.

The result of this investigation is that the contribution of secondary craters even in the kilometer size range is not essential through the whole light interior of Mare Serenitatis, because there exist no other post-mare craters as large as Menelaus and Bessel in the counting area of Mare Serenitatis or its immediate vicinity. One has to be aware that the total number of craters with $D=1$ km is ≈ 100 for the area around Bessel while ≈ 500 for the whole Mare Serenitatis counting area. Less than half of the counting area around Bessel shows a significant contribution of secondary craters. The contribution for the whole Mare Serenitatis counting area of secondary craters is thus $<5\%$. It is clear that the contribution of secondary craters can be neglected in the km-size range for all areas which do not lie in the immediate vicinity of large primary craters. Since we have eliminated secondary craters in the actual counts by application of the herringbone criterion and elongatedness, the contribution of those overlooked must be negligibly small.

From this study we are quite certain that the Mare Serenitatis population is an especially good example of a primary production population. The statistical uncertainty is only $\approx 3\%$ for km-sized craters. All other effects discussed in Section 2 which affect crater populations are excluded by the special choice of the area. Different lava flows may have occurred, but have not greatly affected the population. Only two flooded 'pre-mare' craters have been detected in the counting area.

4.2. Mare crisium

Another example of a largely unchanged production population is the one in the Mare Crisium counting area. Its location is displayed in Table I. Only the eastern part of Mare Crisium has been chosen for counting because the mare filling of the basin does not seem to be homogeneous. The western part shows some large craters (Peirce, Picard, etc.) which seem too frequent and indicate lava flooding to have acted on the crater population of Mare Crisium. These craters are classified as pre-mare craters with respect to the eastern mare counting area (cf. Neukum and König, 1975). The other effects able to affect the size distribution can be excluded analogously to the argumentation in the case of Mare Serenitatis. Flooding may have played a minor rôle, since the distribution shows a slight flattering at larger crater sizes.

The size-frequency distribution of the eastern Mare Crisium crater population is also shown in Figure 6. It has the same characteristics as the Mare Serenitatis population yet is lower in frequency. Thus, the eastern part of the Mare Crisium filling is younger than the average Mare Serenitatis filling.

4.3. Montes apenninus

The best preserved part of the outer ring of the Imbrium basin, the Montes Apenninus has excellently been covered by the Apollo 15 and 17 Metric photography. That is why stereoscopic counting of craters as small as 1.4 km in diameter could be performed in this mountanous area. Region 15-413 was selected for this purpose (Table I). The frequency for craters with diameters $\geqslant 2$ km in region 15-413 together with regions 17-1820, 17-1825 and 17-1823 is given in the same table.

Craters smaller than 1.4 km in diameter have not been counted because of the pronounced relief. Blanketing effects are not likely in this region because it was completely rejuvenated by the Imbrium event and no other subsequent event which could have blanketed this area happened. Flooding by mare basalts has not occurred in the counting area. Crater erosion has not been an effective process for the size of craters counted. They lie far apart from each other and show all rather sharp contours. Secondary craters probably produced by the Imbrium event itself have been easily recognized because of their completely irregular shapes, all elongated in the direction of the center of Imbrium.

4.4. Light plains at the apollo 16 landing site

These plains look very flat and homogenous and thus appear well appropriate for obtaining an unaffected crater size distribution. The counting areas are located as shown in the schematic draft in Table I. The monoscopic counts furnish a smooth regular distribution for crater sizes as small as 1.1 km (Figure 6).

Mass wasting cannot have affected this crater population of because the flatness of the terrain. Secondary craters are present only sporadically, because no large strewn fields exist in this region. Some secondary craters probably stemming from Theophilus have been eliminated.

Subdued craters with diameters smaller than 1 km are frequent. As discussed in Section 2, a population with such an areal crater density is affected by superposition, infilling and abrasion in the size range $\lesssim 0.8$ km (cf. Figure 3). We have not counted craters smaller than 1.1 km in diameter to avoid modification of the population by these effects.

The effects of lava flows and blanketing are difficult to be accounted for. The plains have been interpreted to have formed during the Imbrium excavation by some highly fluidized ejecta material (Eggleton and Schaber, 1972). Other interpretations are an origin by liquefaction (Bastin, 1974) or by local secondary cratering effects (Oberbeck *et al.*, 1974). Whatever their origin is, the surface of the plains which has recorded the craters seems to have formed in a short time span contemporaneous with the Imbrium event. The crater size distribution does not show any irregularity of the type discussed before. The crater frequency is equal to the Apennine frequency within the limits of statistical error.

4.5. Mendeleev

The interior of this large crater is the oldest homogeneous looking plains surface we could find with good coverage by vertical photography. The craters were measured monoscopically after stereoscopic inspection of the whole area. It yields good statistics for the frequency of craters as large as 10 km in diameter.

The counting area given in the schematic draft in Table I also comprises a chain of probably secondary craters (hatched). These craters have been eliminated in counting.

In order to avoid great affection of the measurements by unrecognized secondary craters we have truncated our statistics for small sizes at $D = 3$ km.

Mass wasting cannot be an efficient process in destroying the craters in this area because of its flatness. In this old area, however, the crater diameter measurements may somewhat be affected by mass wasting because material has obviously slumped down the walls of some older looking craters. The diameters are thus enlarged in some cases. This effect is estimated to result in $< 10\%$ deviation in crater frequency. Therefore, we neglect it. Erosion by superposition, abrasion and infilling has only negligibly acted on the craters of the size counted. This has been verified by the visual inspection. The influence of lava flooding and ejecta deposition cannot be evaluated by studies of the terrain. The argumentation follows that for the Apollo 16 LS Light Plains. No irregularity in the distribution can be seen (Figure 6).

We cannot agree with Soderblom and Boyce (1972) who report the same age for the Apollo 16 LS Light Plains (Cayley Plains) and the Mendeleev floor. The interior of Mendeleev is distinctly older because its crater frequency is a factor of 3 higher.

4.6. Mare orientale

This ringed basin is supposed to be the youngest on the Moon (e.g. Stuart-Alexander and Howard, 1970; Hartmann and Wood, 1971). Its interring region between the Rook Mountains and the Cordillera Mountains is a rugged terrain with low elevations

(Head, 1974) well suited for counting craters as small as 3 km in diameter. The counting areas are given in the schematic draft in Table I. The counts of the single areas agree with each other within the statistical limits. The combined size frequency distribution is shown in Figure 6. The frequency lies somewhat below the value for the Montes Apenninus, though most error bars overlap. This is an indication that the Mare Orientale event is somewhat younger than the Mare Imbrium event if no modification of the counting area subsequent to the basin formation took place.

Effects of lava flows on the crater population are eliminated by avoiding mare fillings in selecting the counting areas. Mass wasting cannot have played a rôle for the craters counted because of the flatness of the terrain. Secondary strewn fields of large craters are absent. Erosion of craters is negligible. The craters lie far apart from each other no superposition has occurred.

4.7. Apollo 15 LS

The Apollo 15 Landing Site lies east of Hadley Rille, indicated by the dashed lines in the schematic draft in Table I. The mare area in the small valley on this side is not large enough for sufficiently good statistics. The mare surface on either side of the Rille looks so uniform that we also chose a counting region of Hadley Rille.

The measurements were performed stereoscopically. Thus, it was possible to safely measure frequencies for crater sizes as small as 250 m. The counts for both regions 415.1 and 415.2 agree within the statistical error limits. The counting region is an essentially unblanketed mare surface. Effects of lava flooding and mixing of old with young cratered areas may to a small extent have occurred as already mentioned in Section 2.2. Two craters which lie on the hatched area in the schematic draft in Table I could be 'pre-mare' ones. Secondary cratering has only negligibly occurred in this area, though efficiently farther to the west. The strewn fields of the craters Autolycus and Aristillus may not have reached the counting area to a large extent because of shielding by the surrounding mountains. Mass wasting has not acted because of the flatness of the region. Erosion by superposition, abrasion and infilling has only negligibly affected the craters of the size counted. This has already been shown in Section 2 (Figure 3).

5. Derivation of a Lunar Calibration Crater Size Distribution

The crater populations on the Moon are an image of the mass-velocity-distribution of the bodies that formed the craters. This distribution may be a function of time t. The corresponding crater size distribution be $g(D, t)$. The cumulative cratering rate (corresponding to the cumulative flux of crater-forming bodies) is

$$\phi(D, t) = \int_{D}^{\infty} g(D', t) f(t) \, \mathrm{d}D' ,$$

where $f(t)$ describes the general time dependence of impact frequency. The cumulative

crater frequency, N, then becomes

$$N = \int_{t_i}^{0} \phi \, \mathrm{d}t = \int_{D}^{\infty} \int_{t_i}^{0} g(D', t) \, f(t) \, \mathrm{d}D' \, \mathrm{d}t,$$

where the craters have accumulated between the time t_i (begin of cratering record) and $t=0$ (today).

If the crater size distribution is not dependent on time, then the cumulative frequency becomes

$$\begin{aligned} N &= \int_{D}^{\infty} g(D') \, \mathrm{d}D' \int_{t_i}^{0} f(t) \, \mathrm{d}t \\ &= G(D) \, F(t_i). \end{aligned}$$

For two crater populations N_1 and N_2 with the ages t_1 and t_2, respectively, we then find $(N_1/N_2)=F(t_1)/F(t_2)=c$. Any crater frequency N_2 will result in the frequency N_1 if multiplied by the factor c, which is a number only dependent on the respective ages and not on crater size. Thus, we can normalize the frequencies to each other. On the other hand, if such a normalization procedure is impossible, then the crater size distribution is not independent of time.

In the following it is attempted to perform a normalization of the investigated crater size distributions (Figure 6). As they do not cover the same size range they cannot be normalized to each other at one crater size. So the Mare Serenitatis population which covers the widest size range with the best statistics is taken as a basis. All other distributions are normalized to the distribution of Mare Serenitatis. The normalizing factor c is determined by taking the average ratio of the crater frequencies in the range where they overlap and are statistically best defined. Crater smaller than 0.8 km in diameter were counted only at the Apollo 15 LS. Since the statistics for $D \approx 1$ km is bad for this population and therefore the overlap to the Mare Serenitatis population is insufficient, we have used data from Greeley and Gault (1970) for the completion of the size distribution at small sizes. These data are the only ones published in the size range $D<0.8$ km, which are usable for our purposes. They are given in tabular form with statistical errors. The disadvantage of these data is that they were obtained by technicians with a minimum of scientific bias (quotation) that had the task to count all circular depressions. So the effects discussed in Section 2.1–2.6 modifying primary production populations have not been accounted for. However, those of their data used by us for the completion of the crater size distribution seem to be sufficiently reliable. The counting areas lie in the flat terrain of Oceanus Procellarum far away from strewn fields of large primary impacts. All effects discussed here which modify crater populations except flooding by mare lava are likely not to have acted. The normalized counts which are displayed in Figure 9 together with our own data accordingly show slight flooding-type irregularities at larger crater sizes. However, these irregularities are not well pronounced and the deviations are only slightly outside the ranges

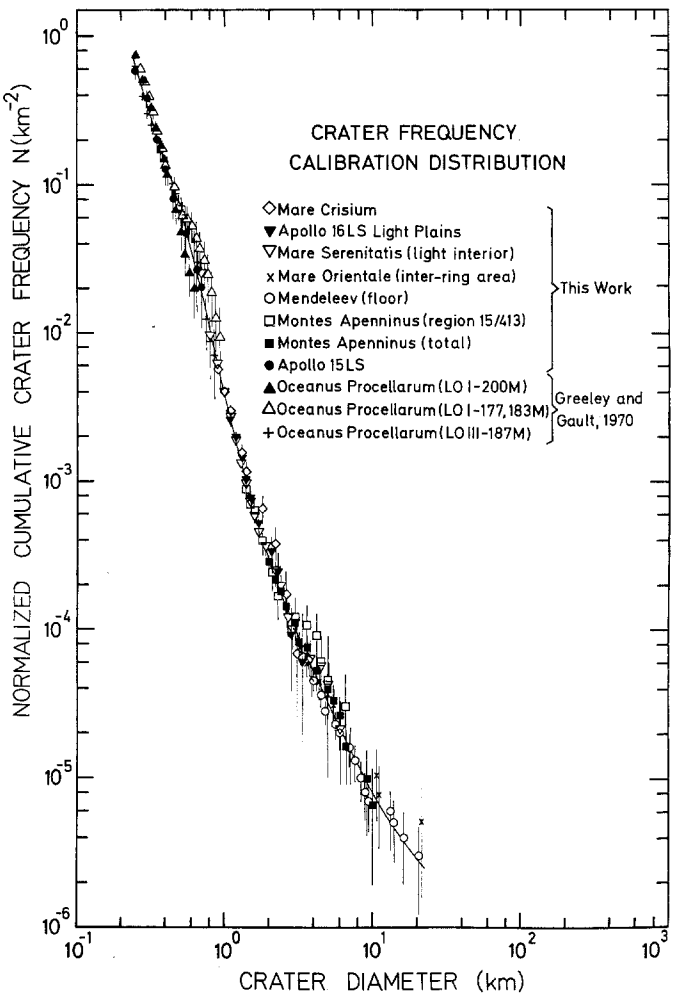

Fig. 9. Cumulative size-frequency distributions of all investigated populations normalized to the frequency of Mare Serenitatis Light Interior. Additionally, data by Greeley and Gault (1970) are used. The solid line represents the polynomial approximation of the calibration size-distribution.

of the statistical errors. Thus, we use these data in spite of a possible deviation from unmodified distributions by $\lesssim 30\%$ in frequency towards the larger craters.

From the normalized distributions in Figure 9 we conclude that all crater populations investigated follow one general distribution behavior within the range of the statistical errors. The obtained size distribution is well defined in the range 1 km $< D <$ 10 km. The oldest populations contributing to it are those of Mendeleev, the Apollo 16 LS Light Plains, and the Montes Apennines. As deduced from Apollo 16 and 15 rocks, the formation age of these areas is $\approx 4 \times 10^9$ yr (e.g. Kirsten and Horn, 1974; Tera *et al.*, 1974) resp. $> 4 \times 10^9$ yr for the floor of Mendeleev according to its higher crater frequency. The populations with the lowest frequency in the range $D > 1$ km is that of

Mare Crisium. By comparison with the Apollo 15 LS frequency, its age is determined to be $\approx 3.3 \times 10^9$ yr (age of the Apollo 15 rocks) (e.g. Papanastassiou and Wasserburg, 1973; Husain, 1974). In the time before 3×10^9 yr ago most of the craters of *any* lunar crater population accumulated during a time span of the order of several 100 million years after exposure (cf. Neukum and König, 1974). Thus, cratering until $\approx 3 \times 10^9$ yr ago contributed to the youngest size distributions. From this we conclude that in the time span between more than 4×10^9 yr ago and about 3×10^9 yr ago the size distribution of lunar crater populations has largely remained constant in the size range $1 \text{ km} < D < 10$ km.

Some uncertainty for the distribution in the size range $1 \text{ km} < D < 3$ km remains for the time interval between the formation of the floor of Mendeleev and 4×10^9 yr, as for this time interval the size distribution is determined only for $D \geqslant 3$ km.

The distributions seem to have been stable even for sizes up to $D \approx 20$ km, but as the statistical error is large minor variations cannot be excluded.

The counts for $D \leqslant 1$ km fall all in the age range between $\approx 3 \times 10^9$ and 3.4×10^9 yr. Thus, we cannot exclude a variation in this size range before 3.4×10^9 yr ago. However, strong variations should not have taken place because such a variation should be seen for sizes somewhat larger than 1 km and should not be limited to sizes $D < 1$ km. If that were so, we should deal with more than one population of crater forming bodies. We should then see a steepening of the distribution rather than a flattening. There is no indication for such a situation in all counts for sizes $D < 1$ km. Thus, it is likely that the distribution has been stable over the whole size range $250 \text{ m} < D < 20$ km between 3×10^9 yr and more than 4×10^9 yr ago.

The curve laid through the points in Figure 9 is a polynomial of 7th degree obtained in a least squares fit. The polynomial has the general form

$$\log N = a_0 + a_1 \log D + a_2 (\log D)^2 + \cdots + a_7 (\log D)^7 .$$

Its coefficients are

$$\begin{aligned} a_0 &= -2.405, & a_4 &= -3.782, \\ a_1 &= -4.333, & a_5 &= -4.871, \\ a_2 &= 0.950, & a_6 &= 7.004, \\ a_3 &= 4.579, & a_7 &= -2.245. \end{aligned}$$

It is valid in the range $300 \text{ m} \leqslant D \leqslant 20$ km.

The mean standard deviation is $\approx 17\%$ for $\log N$. This is equivalent to $\approx 40\%$ for the cumulative frequency N.

A polynomial of 4th degree fits almost equally well the data in the range $0.8 \text{ km} \leqslant D \leqslant 20$ km. Its coefficients are

$$\begin{aligned} a_0 &= -2.429, & a_3 &= -0.312, \\ a_1 &= -4.193, & a_4 &= -0.113. \\ a_2 &= 1.944, \end{aligned}$$

The mean standard deviation is $\approx 11\%$ for $\log N$ equivalent to $\approx 25\%$ for N. It should be emphasized that the accuracy for comparing crater frequencies through the polynomial expression is highest in the range 0.8 km $\leqslant D \leqslant$ 3 km. The average uncertainty is $< 10\%$. The distribution is steepest there, and normally craters are preferentially measured in this size range which leads to good statistics. On the other hand, highest accuracy in crater frequency measurements in this range is mandatory. An error of 20% in diameter determination e.g. leads to more than 100% error in crater frequency.

It is possible that the calibration distribution should be somewhat steeper in the range $D < 0.8$ km since as discussed before the distributions taken from Greeley and Gault (1970) show slight indications of irregularities around $D = 1$ km. They could be due to affections of the populations by lava flows which may have flattened the distribution somewhat.

In summary, we have found a size frequency calibration distribution which represents the general distribution of lunar craters for regions with formation ages between 3 and more than 4×10^9 yr. It is valid with an uncertainty better than 50% in the diameter range 300 m $\leqslant D \leqslant$ 20 km. It is most well defined in the range 0.8 km $\leqslant D \leqslant$ $\leqslant$ 3 km with an uncertainty $< 10\%$ and reasonably well in the range 0.8 km $\leqslant D \leqslant$ 10 km with an uncertainty $< 25\%$.

The age differences of individual regions are mathematically expressed by an additive term in the distribution, $\log F(t_i)$. The general polynomial relationship is, therefore, of the form

$$\log N = a_0 + a_1 \log D + a_2 (\log D)^2 + \cdots + a_7 (\log D)^7 + \log F(t_i).$$

In our normalization procedure, $F(t_i)$ is arbitrarily set equal to 1 for an age corresponding to the Mare Serenitatis frequency.

The polynomial expression for the logarithm of crater frequency can be cast into a form analogous to simple power law distributions, $N \sim D^{\alpha}$, found in the literature. The exponent, α, is then, however, not a constant, but a function of D. This frequency relationship becomes

$$N = A D^{\alpha(D)} F(t_i),$$

where

$$A = 10^{a_0}$$

and

$$\alpha(D) = a_1 + a_2 (\log D) + a_3 (\log D)^2 + \cdots a_7 (\log D)^6.$$

In Figure 10 we compare the crater frequency calibration distribution with distributions reported in the literature, (a) $N \sim D^{-2.9}$ (Shoemaker *et al.*, 1970), (b) $N \sim D^{-2}$ (Hartmann and Wood, 1971), and (c) $N \sim D^{-1.8}$ (Baldwin, 1972). Shoemaker *et al.*'s distribution, $N \sim D^{-2.9}$, given for the size range 100 m $\leqslant D < 3$ km is approximately consistent with the one derived in this paper in the range 250 m $< D <$ 800 m, but seriously deviates for $D >$ 800 m. For $D = 2$ km, it would lead to errors of about a factor of 5.

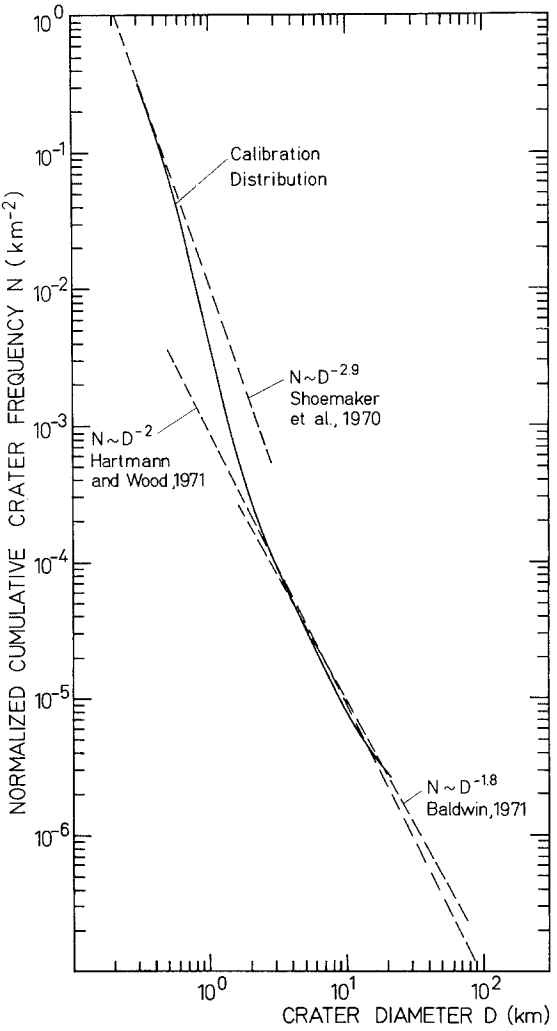

Fig. 10. Comparison of the derived crater size-frequency calibration distribution with distributions found by different authors. These straight distributions are roughly normalized to the calibration distribution polynomial in the range where the approximation is best. They are drawn in the range of reported validity.

Baldwin's distribution, $N \sim D^{-1.8}$, given for the size range 1.6 km $\leqslant D <$ 100 km is in good approximate agreement with our calibration distribution in the range 3 km $< D <$ 20 km. An extrapolation to only little smaller sizes such as 1.6 km leads to errors of about a factor of 2.

Hartmann and Wood's distribution $N \sim D^{-2}$, very grossly averages the real conditions. It is reported to be valid in the size range 500 m $\leqslant D \leqslant$ 100 km. The agreement with our calibration distribution or the distribution given by Baldwin is good in the size range 3 km $< D <$ 20 km. For smaller sizes, however, it leads to errors up to a factor of 10.

7. Conclusions

We have shown that there exists one general size distribution for lunar impact crater production populations which formed on surfaces with formation ages between ≈ 3 and more than 4 Aeons. This leads us to the conclusion that either the mass-velocity-distribution of the crater forming bodies was constant during that time span or separate variations in the mass distribution and the velocity distribution compensated each other with respect to the resulting crater sizes.

The importance of this calibration size distribution is that over a large range of crater sizes it allows a comparison of crater frequencies of lunar areas when the comparison of crater frequencies in the same size range is not possible because: statistics are insufficiently good; type of area, quality of photomaterial, and processes modifying crater populations in different size ranges may restrict measurements at certain crater sizes. The calibration size distribution given in polynomial approximation allows the comparison of any lunar crater populations by measuring their crater frequencies at the best defined size ranges.

Deviations from the calibration size distribution are strongly suggestive of the existence of processes such as surface lava flows, blanketing by ejecta, superposition, infilling, and abrasion of craters, mass wasting, and the contribution of secondary and volcanic craters, which have acted on the primary impact crater populations. Discrepancies in crater frequencies of the same populations reported in the literature may be due to the fact that previously these processes have not been accounted for adequately. Further inconsistencies may have resulted. from inadequate approximations of the lunar impact crater size distributions.

In summary, application of the derived calibration distribution should help to resolve many discrepancies in the determination of relative ages of lunar provinces by crater frequency measurements. Additionally, complex histories of individual regions may be revealed by studying the deviations of the distributions from the regular one.

Acknowledgment

We thank the Planetology Program Office, NASA Headquarters, Washington, D.C. and the Lunar Science Institute, Houston, for providing the photographic material for our studies.

Assistance and advice by our colleagues of the Cosmochemistry department of the Max-Planck-Institut für Kernphysik, Heidelberg, is gratefully acknowledged.

References

Baldwin, R. B.: 1949, *The Face of the Moon*, University of Chicago Press, Chicago, Ill., U.S.A.
Baldwin, R. B.: 1963, *The Measure of the Moon*, University of Chicago Press, Chicago, Ill., U.S.A.
Baldwin, R. B.: 1971, *Icarus* **14**, 36.
Bastin, J. A.: 1974, *The Moon* **10**, 143.
Bloch, M. R., Fechtig, H., Gentner, W., Neukum, G., and Schneider, E.: 1971, *Proc. 2nd Lunar Sci. Conf., Geochim. Cosmochim. Acta, Suppl. 2*, **2**, 2639.

Chapman, C. R. and Heafner, R. R.: 1967, *J. Geophys. Res.* **72**, 549.
Eggleton, R. E. and Schaber, G. G.: 1972, *Apollo 15 Preliminary Science* Report, 29-7.
Gault, D. E.: 1970, *Radio Science* **5**, 273.
Greeley, R. and Gault, D. E.: 1970, *The Moon* **2**, 10.
Grudewicz, E. B.: 1973, *Nature* **241**, 186,
Hartmann, W. K.: 1970, *Icarus* **13**, 299.
Hartmann, W. K.: 1972, *Astrophys. Space Sci.* **17**, 48
Hartmann, W. K. and Wood, C. A.: 1971, *The Moon* **3**, 3.
Head, J. W.: 1974, *The Moon* **11**, 327.
Husain, L.: 1974, *J. Geophys. Res.* **79**, 2588.
Kaula, W. M., Schubert, G., Lingenfelter, R. E., Sjogren, W. L., and Wollenhaupt, W. R.: 1973, *Proc. 4th Lunar Sci. Conf., Suppl. 4, Geochim. Cosmochim. Acta* **3**, 2811, MIT Press.
Kirsten, T. and Horn, P.: 1974, 'Chronology of the Taurus-Littrow Region III: Ages of Mare Basalts and Highland Breccias and Some Remarks about the Interpretat n of Lunar Highland Rock Ages', to be published in *Proc. 5th Lunar Sci. Conf., Geochim, Cosmochim. Acta, Suppl. 5.*
LAC Charts: 1962, *Astronautical Chart and Information Center*, United States Air Force, St. Louis, Missouri.
Lunar Planning Chart: 1972, *National Aeronautics ane Space Administration.*
Marcus, A. H.: 1964, *Icarus* **3**, 460.
Marcus, A. H.: 1966, *Icarus* **5**, 165.
McGetchin, T. R., Settle, M., and Head, J. W.: 1973, *Earth Planetary Sci. Letters* **20**, 226.
Moore, H. J.: 1964, *Density of Small Craters on the Lunar Surface*, U.S. Geol. Surv. Astrogeol. Stud. Ann. Prog. Rep., Part D, Government Print. Off., Washington D.C., p. 34.
Neukum, G. and Dietzel, H.: 1971, *Earth Planetary Sci. Letters* **12**, 59.
Neukum, G. and Horn, P.: 1974, *Effects of Lava Flows on Lunar Crater Population*, to be published.
Neukum, G. and König, B.: 1975, 'Age Determination by Lunar Crater Size Frequency Measurements', to be published in *The Moon.*
Neukum, G., Schneider, E., Mehl, A., Storzer, D., Wagner, G. A., Fechtig, H., and Bloch, M. R.: 1972, 'Lunar Craters and Exposure Ages Derived from Crater Statistics and Solar Flare Tracks', *Proc. 3rd Lunar Sci. Conf., Suppl. 3, Geochim. Cosmochim. Acta* **3**, 2793, MIT Press.
Oberbeck, V. R. and Morrison, R. H.: 1974, *The Moon* **9**, 415.
Oberbeck, V. R., Hörz, F., Morrison, R. H., Quaide, W. L., and Gault, D. E.: 1974, *Lunar Science V*, 568, Lunar Science Institute, Houston.
Öpik, E. J.: 1960, *Monthly Notices Roy. Astron. Soc.* **120**, 404.
Papanastassiou, D. A. and Wasserburg, G. J.: 1973, *Earth Planetary Sci. Letters* **17**, 324.
Schaber, G. G.: 1973, *Proc. 4th Lunar Sci. Conf., Geochim. Cosmochim. Acta, Suppl. 4*, **1**, 73.
Shoemaker, E. M., Hackman, R. J., and Eggleton, E. R.: 1962, *Adv. Astron. Sci.* **8**, 70.
Shoemaker, E. M.: 1970, 'Origin of Fragmental Debris on the Lunar Surface and the History of the Bombardment of the Moon', paper presented at I Seminario de Geologia Lunar, University of Barcelona.
Shoemaker, E. M., Batson, R. M., Bean, A. L., Conrad, C., Jr., Dahlem, D. H., Goddard, E. N., Hait, M. H., Larson, K. B., Schaber, G. G., Schleicher, D. L., Sutton, R. L., Swann, G. A., and Waters, A. C.: 1970, NASA SP-235, 113.
Soderblom, L. A.: 1970, *J. Geophys. Res.* **75**, 2655.
Soderblom, L. A. and Boyce, J. M.: 1972, *Apollo 16 Preliminary Science Report*, 29-3.
Stöffler, D.: 1974, personal communication.
Stuart-Alexander, D. and Howard, K.: 1970, *Icarus* **12**, 440.
Tera, F., Papanastassiou, D. A., and Wasserburg, G. J.: 1974, *Earth Planetary Sci. Letters* **22**, 1.
Trask, N. J.: 1966, 'Size and Spatial Distribution of Craters Estimated from Ranger Photographs', Jet Propul. Lab. Tech. Rep. 32-700, Pasadena, Calif., p. 252.
Walker, E. H.: 1967, *Icarus* **7**, 233.